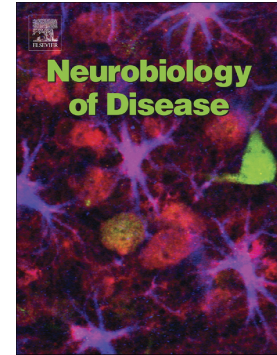


## Accepted Manuscript

Phase-amplitude coupling and epileptogenesis in an animal model of mesial temporal lobe epilepsy

Soheila Samiee, Maxime Lévesque, Massimo Avoli, Sylvain Baillet



PII: S0969-9961(18)30040-8  
DOI: doi:[10.1016/j.nbd.2018.02.008](https://doi.org/10.1016/j.nbd.2018.02.008)  
Reference: YNBDI 4115  
To appear in: *Neurobiology of Disease*  
Received date: 18 October 2017  
Revised date: 9 February 2018  
Accepted date: 21 February 2018

Please cite this article as: Soheila Samiee, Maxime Lévesque, Massimo Avoli, Sylvain Baillet, Phase-amplitude coupling and epileptogenesis in an animal model of mesial temporal lobe epilepsy. The address for the corresponding author was captured as affiliation for all authors. Please check if appropriate. Ynbdi(2017), doi:[10.1016/j.nbd.2018.02.008](https://doi.org/10.1016/j.nbd.2018.02.008)

This is a PDF file of an unedited manuscript that has been accepted for publication. As a service to our customers we are providing this early version of the manuscript. The manuscript will undergo copyediting, typesetting, and review of the resulting proof before it is published in its final form. Please note that during the production process errors may be discovered which could affect the content, and all legal disclaimers that apply to the journal pertain.

# **Phase-Amplitude Coupling and Epileptogenesis in an Animal Model of Mesial Temporal Lobe Epilepsy**

**Soheila Samiee<sup>1</sup>, Maxime Lévesque<sup>1</sup>, Massimo Avoli<sup>1,2</sup>, Sylvain Baillet<sup>1,\*</sup>**

**<sup>1</sup> Montreal Neurological Institute, and Department(s) of Neurology & Neurosurgery  
and of <sup>2</sup> Physiology, McGill University, Montreal, QC, Canada.**

Running title: Phase-amplitude coupling and epileptogenesis

Manuscript pages:	31
Number of Figures:	5
Number of words in Abstract:	298
Number of words in Introduction:	406
Number of words in Discussion:	1323

\*Correspondence to: Sylvain Baillet  
McConnell Brain Imaging Centre  
Montreal Neurological Institute, NW107  
McGill University, 3801, University Street,  
Montreal, Qc H3A2B4  
Canada  
sylvain.baillet@mcgill.ca

**Abstract**

Polyrhythmic coupling of oscillatory components in electrophysiological signals results from the interactions between neuronal sub-populations within and between cell assemblies. Since the mechanisms underlying epileptic disorders should affect such interactions, abnormal level of cross-frequency coupling is expected to provide a signal marker of epileptogenesis. We measured phase-amplitude coupling (PAC), a form of cross-frequency coupling between neural oscillations, in a rodent model of mesial temporal lobe epilepsy. Sprague-Dawley rats ( $n = 4$ , 250-300 g) were injected with pilocarpine (380 mg/kg, i.p) to induce a status epilepticus (SE) that was stopped after 1 h with diazepam (5 mg/kg, s.c.) and ketamine (50 mg/kg, s.c.). Control animals ( $n = 6$ ) did not receive any treatment. Three days after SE, all animals were implanted with bipolar electrodes in the hippocampal CA3 subfield, entorhinal cortex, dentate gyrus and subiculum. Continuous video/EEG recordings were performed 24/7 at a sampling rate of 2 kHz, over 15 consecutive days. Pilocarpine-treated animals showed interictal spikes ( $5.25 (\pm 2.5)$  per minute) and seizures ( $n=32$ ) that appeared  $7 (\pm 0.8)$  days after SE. We found that CA3 was the seizure onset zone in most epileptic animals, with stronger ongoing PAC coupling between seizures than in controls (Kruskal-Wallis test:  $\chi^2 (1,36) = 46.3$ , Bonferroni corrected,  $p < 0.001$ ). Strong PAC in CA3 occurred between the phase of slow-wave oscillations ( $<1$  Hz) and the amplitude of faster rhythms (50–180 Hz), with the strongest bouts of high-frequency activity occurring preferentially on the ascending phase of the slow wave. We also identified that cross-frequency coupling in CA3 ( $\rho = 0.44$ ,  $p < 0.001$ ) and subiculum ( $\rho = 0.41$ ,  $p < 0.001$ ) was positively correlated with the daily number of seizures. Overall, our study demonstrates that cross-frequency coupling may represent a biomarker in epilepsy and suggests that this methodology could be transferred to clinical scalp EEG recordings.

**Keywords:** temporal lobe epilepsy; pilocarpine; cross-frequency phase-amplitude coupling; neural oscillations; CA3; seizures.

**Conflict of interest**

None of the authors has any conflict of interest to disclose.

**Acknowledgments**

The authors thanks Dr. Charles Behr for his help in surgical preparation of the animals used in this study that was supported by the Canadian Institutes of Health Research (CIHR grants 8109 and 74609 to M.A.). S.S. acknowledges the support from McGill University Integrated Program in Neuroscience. S.B. was supported a Discovery Grant from the National Science and Engineering Research Council of Canada (436355-13), the NIH (2R01EB009048-05) and a Platform Support Grant from the Brain Canada Foundation (PSG15-3755).

## 1 Introduction

Mesial temporal lobe epilepsy (MTLE) is a focal epileptic disorder characterized by recurrent seizures arising from limbic structures such as the hippocampus, the amygdala or entorhinal cortex (Spencer and Spencer, 1994; Salanova et al., 1994; Engel, 1996; Gloor, 1997). Seizures occur following a latent period of several years after an initial brain insult such as status epilepticus (SE), traumatic brain injury, encephalitis or febrile convulsions (Cendes et al., 1993; French et al., 1993). Approximately one-third of MTLE patients are unresponsive to antiepileptic drugs (Jallon, 1997; Wiebe et al., 2001; Engel et al., 2012): MTLE is one of the most refractory forms of focal epilepsy. Surgical resection of the epileptic tissue remains the only therapeutic alternative (Salanova et al., 1994; Wiebe, 2004; Blume and Parrent, 2006, Engel et al., 2012), provided that the seizure onset zones (SOZ) are correctly localized. The identification of the SOZ is challenging, in particular since it is mainly obtained from inter-ictal electrophysiological data. Therefore, the present study emphasizes the possible role of cross-frequency coupling between oscillatory components of neural signal as a signal marker of epilepsy.

Cross-frequency coupling is a phenomenon of inter-dependence between brain rhythms of different frequencies. It has been observed in multiple preparations in rodents and humans, using a variety of electrophysiology techniques, from invasive recordings to scalp magnetoencephalography and source imaging (Canolty and Knight, 2010; Florin and Baillet, 2015; Baillet 2017). Phase-amplitude coupling (PAC) is a type of cross-frequency coupling where the phase of slow oscillations modulates the amplitude of faster rhythms (Tort et al., 2010). Invasive recordings in rodent models and epileptic patients revealed that PAC was stronger in the seizure onset zones (Amiri et al., 2016; Nariai et al., 2011; Weiss et al., 2013; Ibrahim et al., 2014; Guirgis et al., 2015; Weiss et al., 2016), and during the pre-ictal and ictal phases (Colic et al., 2013; Alvarado-Rojas et al., 2014; Zhang et al., 2017).

We used here the pilocarpine animal model of MTLE (Curia et al., 2008) to investigate the possible association between expressions of PAC and ictogenesis in temporal lobe regions. We measured PAC between the phase of slow oscillations (slow-wave in the delta band: 0.18–4 Hz) and the amplitude of faster rhythms (beta to ripple band: 20–250 Hz) in controls and in pilocarpine-treated rats. Our results

indicate a strong association between PAC signal markers (coupling strength and phase) and seizure activity in temporal lobe regions in this rodent model of MTLE.

## 2 Material and Methods

### 2.1 Animal preparation

The methods for animal preparation have been described in detail previously (Behr et al. 2015; 2017; Lévesque et al. 2011; 2012; Salami et al. 2014). All procedures were approved by the Canadian Council on Animal Care and the Institutional Animal Care Committee of McGill University. Every effort was made to minimize the number of animals used and their suffering.

Male Sprague-Dawley rats (250-300 g; Charles-River (St-Constant, QC, Canada)) were let habituate for 72 h before pilocarpine treatment. Animals were housed at 22 ( $\pm$  2) °C under 12 h light/12 h dark cycle with food and water *ad libitum*. Scopolamine methylnitrate (1 mg/kg i.p.; Sigma-Aldrich, Canada) was administered 30 min before pilocarpine hydrochloride (380 mg/kg, i.p.; Sigma-Aldrich, Canada) to induce a status epilepticus (SE). SE was terminated after 1 h using diazepam (5 mg/kg, s.c.; CDMV, Canada) and ketamine (50 mg/kg, s.c.; CDMV, Canada) (Martin and Kapur, 2008). Three days after SE, rats underwent surgery for the implantation of bipolar depth electrodes. Rats were anesthetized with isoflurane (3%) in 100% O<sub>2</sub>. Four bipolar electrodes (20-30 k $\Omega$ ; 4-10 mm length; distance between exposed tips: 500  $\mu$ m, MS303/2-B/spc, Plastics One, VA, USA) were implanted in the CA3 subfield of the ventral hippocampus (AP: -4.4, ML: -4, DV: -7.8), the medial entorhinal cortex (EC) (AP: -6.6, ML: -5.2, DV: -6.8); the ventral subiculum (Sub) (AP: -6.8, ML: +4, DV: -6), and the dentate gyrus (DG) (AP: -4.4, ML: +2.4, DV: -3.4) (Paxinos and Watson, 1998). The CA3 region and the EC were implanted on the right side, the subiculum and the dentate gyrus were implanted on the left side. Four stainless steel screws (2.4 mm length) were fixed to the skull bone and electrodes were fastened to the skull with dental cement. A fifth electrode was used as reference, after removal of insulating material, and placed under the frontal bone. Ketoprofen (5 mg/kg, s.c. Merail, Canada), buprenorphine (0.01-0.05 mg/kg, s.c. repeated every 12 h; CDMV, Canada) and 2 ml of 0.9% sterile saline were given up to 3 days after surgery.

After surgery, continuous EEG-video recordings were performed 24h/day. EEG signals were amplified via an interface kit (Mobile 36ch LTM ProAmp, Stellate, Montreal, QC, Canada), and sampled at 2 kHz. Infrared cameras were used to record day/night video files that were time-stamped for integration with the electrophysiological data using monitoring software (Harmonie, Stellate, Montreal, QC, Canada). Throughout the recordings, animals were placed under controlled conditions ( $22\pm 2$  C, 12-hour light/dark schedule) and provided with food and water *ad libitum*.

## 2.2 Analysis of seizures and seizure onset zones

Seizures were identified with the ICTA-D seizure detector (Harmonie; Stellate) and seizure onset zones were identified according to Lévesque et al. (2012). Briefly, the first region showing fast activity (5-20 Hz) was considered as the seizure onset zone. The seizure onset zone was defined according to previous published reports of animal models of MTLE (Levesque et al., 2012; 2015; Behr et al., 2017; Toyoda et al., 2015; Karunakaran et al., 2016) and clinical studies (Wendling et al., 2010; 2013). Seizures were categorized into four types: (1) “CA3” seizures initiated in CA3; (2) “CA3+” seizures originated from CA3 and another region simultaneously; (3) “multi” seizures originated simultaneously at all recording sites; and (4) “CA3-” seizures did not involve CA3.

## 2.3 Extraction of NREM sleep epochs

Periods of sleep characterized by non-rapid eye movement (NREM) were defined by muscular hypotonia (curled body position) and prominent delta activity (1-6 Hz). NREM segments were selected from the video recordings at least 1 h from the last/next seizure episode (Levesque et al., 2011; Salami et al., 2014). One 10-min artefact-free epoch of NREM sleep was selected in each animal for each day of recording. The data selected consisted of 137 epochs from 6 controls and 4 epileptic animals. These epochs were exported to Matlab (The Mathworks, Natick, MA) and analysed off-line. Power line contamination (main and harmonics) was reduced using notch filters with default settings available from Brainstorm, a free open-source application for electrophysiology signal analysis (Tadel et al., 2011).

Figure 1A shows samples of wide-band recordings from all recorded regions, in a control and in an epileptic animal. Power spectrum density analysis revealed that slow oscillations were recorded in all four regions (Fig. 1B). The frequency peak of the slow oscillation was extracted in each animal, after compensation of the  $1/f$  decrease of the power spectral density, using Brainstorm. We call here *slow-wave oscillations*, oscillatory signals below 1 Hz. No substantial differences in slow oscillatory power were found between the control and epileptic groups, except in the dentate gyrus, where slow oscillatory power was higher in controls (Kruskall-Wallis test:  $p < 0.001$  – Fig. 1C).



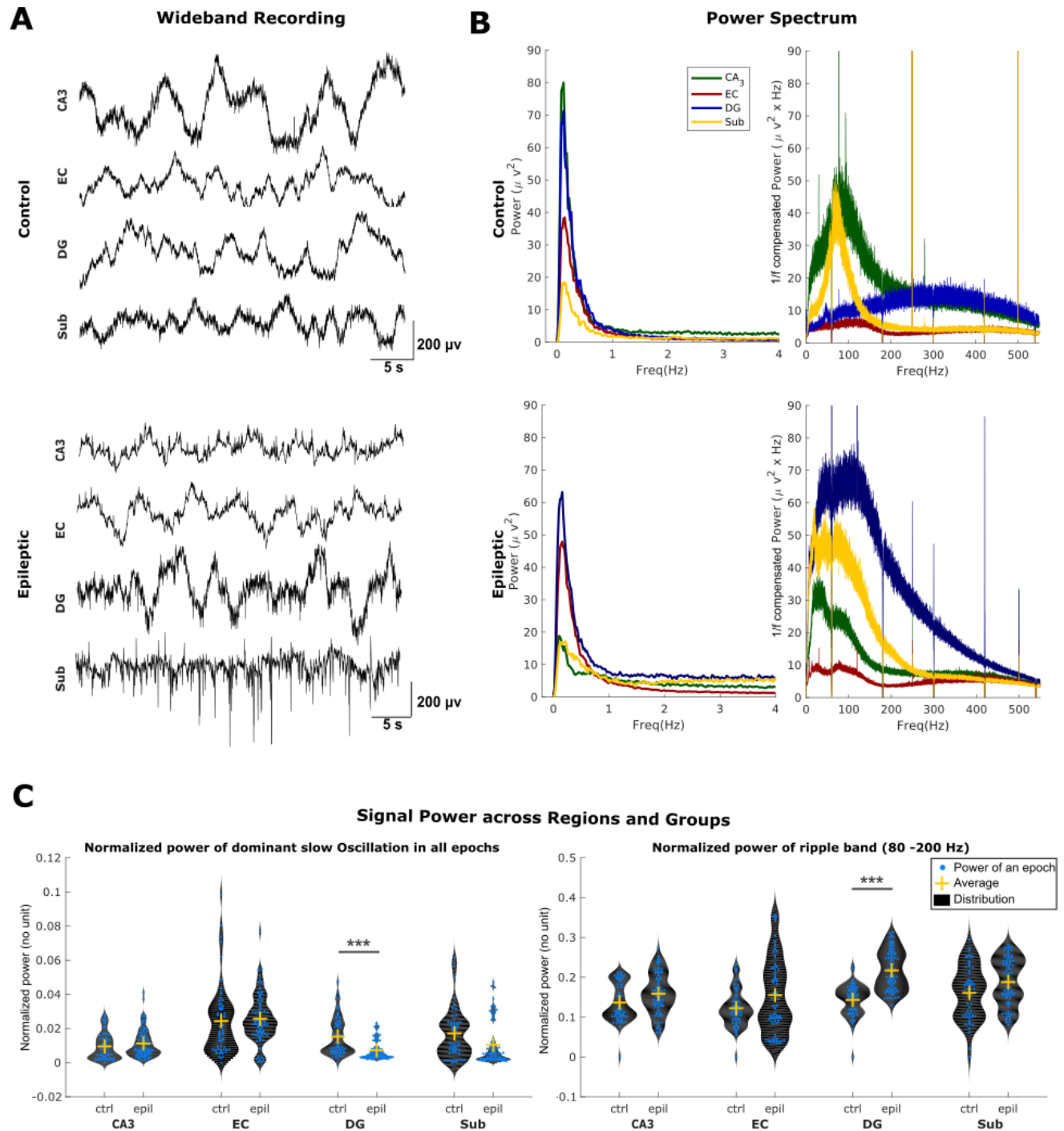


**Figure 1. Typical recordings from control and epileptic animals** **A:** Wideband sample recordings from a control (top) and from an epileptic animal (bottom). **B:** Power spectral density plots extracted from the same animals shown in **A**, after compensation of  $1/f$  decrease: note a strong peak below 1 Hz at all recording sites in both animals. **C:** Regional distribution of normalized signal power of dominant slow oscillation (left), and of the ripple band: 80 – 200 Hz (right) across epochs. No differences were found between groups, except in DG, where slow activity was weaker and ripple-band activity was stronger in the epileptic group (Kruskall-Wallis test, d.o.f: 136,  $p < 0.001$ , Bonferroni corrected for multiple comparisons). Comparisons between regions for each group is reported in Section 3.2.

We standardized the definition of peaks and troughs of the observed slow oscillations across animals and recording sites. The rationale is that the polarity of the oscillatory cycles collected from the bipolar recordings depends on uncontrolled factors, such as the electrode location with respect to the current flow of neural generators, which varies across sites and animals. We followed the recommendations from Ellenrieder et al. (2016), whereby the peaks of slow oscillations are defined as the extrema of the half oscillatory cycles concomitant with stronger beta-gamma band activity. We therefore extracted the instantaneous amplitude of the recordings in the 20-80 Hz band using the Hilbert transform also available in Brainstorm. We then identified the half cycle of the dominant slow oscillation with strongest beta-gamma amplitude. In each animal and at each recording site, the polarity of the signal was flipped if the peak of beta-gamma activity did not correspond to a positive half-cycle of the slow oscillation.

## 2.4 Phase-amplitude coupling analysis

PAC is the modulation of the amplitude of an oscillation at frequency  $f_A$  (frequency for amplitude) along the phase of a slower rhythm of frequency  $f_P$  (frequency for phase), with  $f_P < f_A$ . The frequencies  $f_A$  and  $f_P$  of the dominant PAC mode need to be identified in each animal and at each recording site, together with their coupling strength. The frequency ranges of interest for identifying  $f_A$  and  $f_P$  were set to 0.18–4 Hz for the slow oscillation, and 20–250 Hz for the faster components. We used a recent time-resolved PAC measure (tPAC) with sliding time windows length of 18 s, also available in Brainstorm

(Samiee & Baillet, 2017). Briefly (see Samiee and Baillet (2017) for methodological details), the tPAC method proceeds as follows: at each recording site, the instantaneous amplitude  $A_{f_A}(t)$  of fast oscillatory activity is extracted over sliding time windows (18 s long) using the Hilbert transform in multiple sub-bands of the 20–250 Hz frequency range of interest. The periodogram of  $A_{f_A}(t)$  and of the original signal are then obtained and the frequency for phase  $f_P$  is identified as the common peak of maximum amplitude in both power spectra, if any. If no common peak frequency is found, the conclusion is the absence of PAC in the time series. The electrode signal is then bandpass filtered around  $f_P$ , and its instantaneous phase ( $\phi_{f_P}(t)$ ) is extracted, also using the Hilbert transform. PAC coupling strength is measured via Euclidean averaging of the complex signal vectors of amplitude  $A_{f_A}(t)$  and phase  $\phi_{f_P}(t)$  across time, divided by the average signal power at frequency  $f_A$ . This procedure was repeated for all time-windows and all high-frequency sub-bands.

Large-band spiking signal waveforms can bias PAC estimates. For this reason, interictal spikes were identified in all recordings using a custom detection process: for all 10-min trials, spike events were marked when electrode signals crossed an amplitude threshold of 4 standard deviations above the signal average. All detected events were visually inspected, and events possibly produced by movement artefacts were excluded. We quantified the density of interictal spike occurrences along the phase of slow-wave oscillations, as a preferred phase concentration of spiking activity would bias PAC scores. The phase of slow oscillations was extracted from the Hilbert transform of data signals filtered in the band of interest. As detailed in the Results section, we found that spike occurrences were uniformly distributed (see Fig. 2) along the phase of the  $f_P$  oscillation, and concluded they did not produce spurious PAC activity. For this reason, data epochs containing interictal spike events were not discarded from the data presented below.

Another possible confound in PAC measures is their sensitivity to the harmonics of non-sinusoidal waveforms of the  $f_P$  oscillations (Gerber et al., 2016; Lozano-Soldevilla et al., 2016; Cole and Voytek, 2017). We followed the guidelines suggested by Jensen et al. (2016) and verified there was no correlation between the respective time variations of the amplitude of  $f_P$  oscillations and of the PAC coupling strength.

## 2.5 Statistical analysis

We used inferential statistics to assess the significance of differential effects in power, PAC coupling strength, and preferred PAC phase patterns in all 4 recorded regions, between control and epileptic animals. We used non-parametric Kruskal-Wallis tests for assessing the main effect, and Dunn's tests as post-hoc. We used parametric Watson-Williams multi-sample tests with equal means, the circular equivalent of one-way ANOVA, for the analysis of phase effects. We determined whether the distribution of phase angles of the  $f_P$  oscillations when interictal spikes occurred departed from uniformity using Rayleigh's test. A larger z-value of Rayleigh's statistics would have been indicative of interictal spikes occurring at a preferred phase of the slow-wave oscillations. Phase angles were computed between 0 and 360 degrees, where 0 (respectively 180) corresponded to the peak (respectively the trough) of the oscillatory signal, as defined above. For correlation between measures we used Pearson correlation. Bonferroni corrections for multiple comparisons were applied in all tests.

## 3 Results

### 3.1 Seizures and interictal spikes

Pilocarpine-treated animals showed recurrent spontaneous seizures, on average  $7 (\pm 0.8)$  days after SE. The definition of the seizure onset zone was based on a total of 32 seizures recorded across all animals. As previously reported (Lévesque et al. 2012), CA3 was involved as a seizure onset zone in most cases across all epileptic animals (CA3 = 7, CA3+ = 7, CA3- = 3, widespread = 15, Fig. 2A). We collected a maximum of 7 seizures per day per animal in the epileptic group. The seizures occurred in clusters, consistent with several previous reports concerning the pilocarpine animal model of MTLE (Bortel et al., 2010; Levesque et al., 2011; 2015; Goffin et al., 2007; Pitsch et al., 2017). Interictal spikes were observed in all recorded regions. Control animals did not show interictal spikes or seizures.

We recorded an average of 5.25 ( $\pm 2.5$ ) interictal spikes per minute in all epileptic animals. The number of interictal spikes was significantly different between regions (Kruskal-Wallis test:  $\chi^2$  (3, 308) = 128.24,  $p < 0.001$ ). As previously reported (Behr et al., 2015; Levesque et al., 2015) interictal spikes occurred at higher rates in CA3 and subiculum, than in EC or DG (post-hoc: Dunn's tests,  $p < 0.001$ , Fig. 2B). CA3 and subiculum interictal spike rates were not significantly different ( $p = 0.37$ ).

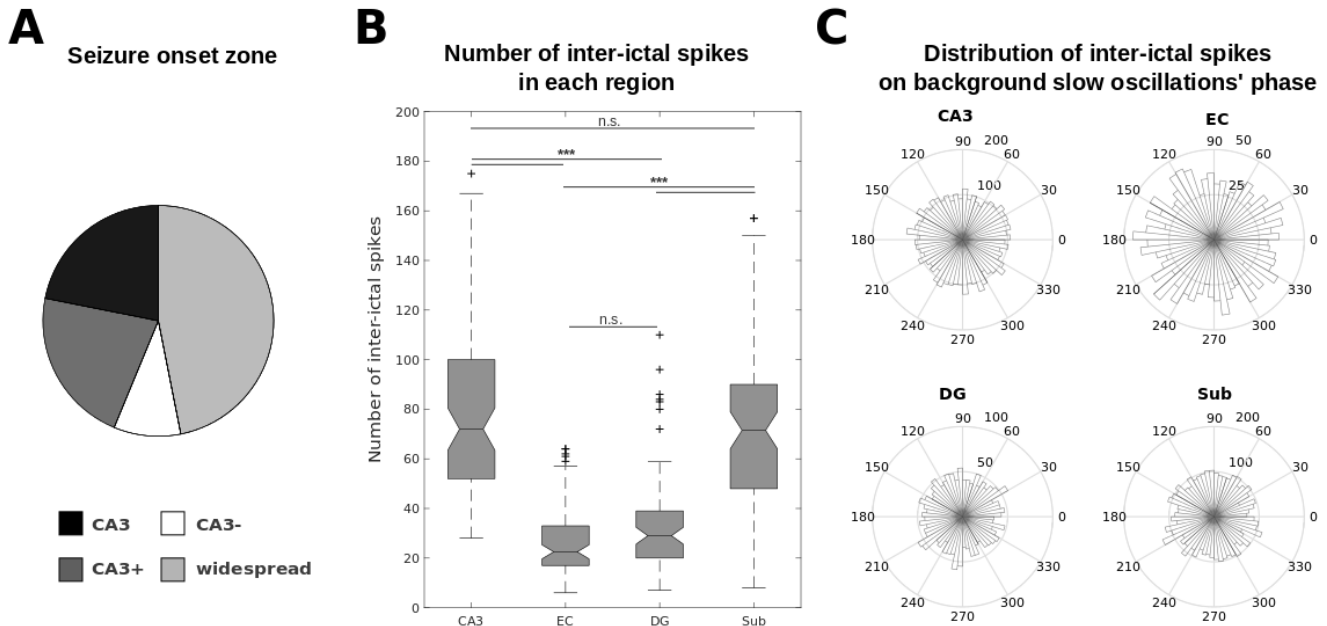


**Figure 2. Seizure onset zone and interictal spikes in epileptic animals.** **A:** Pie chart showing the distribution of seizure onset zones in epileptic animals. CA3 was mostly involved as a seizure onset zone. **B:** Number of interictal spikes at each recording site (\*\*\*:  $p < 0.001$ ). CA3 and subiculum showed the highest rate of interictal spikes compared to EC and DG. **C:** Polar plots showing the distribution of interictal spikes relatively to the phase of background slow-wave oscillations: the phase distribution of the data was not significantly different from a uniform distribution (Rayleigh's test for non-uniformity,  $p > 0.10$ ).

Bandpass filtering of interictal spikes produce fast oscillatory artefacts, which may bias PAC measures if spiking activity occurs at a preferred phase of background slow-wave oscillations. We verified this was not the case in our data: the distribution of interictal spikes occurrences did not show clustering at a preferred phase of the slow oscillations (Fig. 2C). This verification was derived considering two low-frequency ranges for phase-driving slow oscillations: 1) the band of interest for  $f_P$

(0.18 – 4 Hz), and 2) all frequencies below 2 Hz where PAC was strongest in all regions (see Fig. 3C). No spike clustering was found with either of the low-pass settings (Rayleigh's test for non-uniformity,  $p > 0.10$ ). We therefore proceeded with performing PAC analysis over the entire 10-min time-period, without excluding interictal spikes.

### 3.2 Power effect: slow-wave oscillations and ripple band

The presence of a dominant slow oscillation in the band of interest for  $f_P$  is a safeguard condition for valid (not spurious) PAC detection (Aru et al., 2015). Dominant slow oscillations ( $< 1$  Hz) were observed in all epochs in all recorded regions, both in controls and in epileptic animals (Fig. 1). To investigate possible influence of slow-oscillatory signal power on the estimation of PAC coupling strength, we measured the relative power of the dominant slow oscillations with respect to the total power spectrum of the signal at each recording site and in each epoch. In comparison of groups, difference in relative signal power was only found in DG (Kruskall-Wallis test, Bonferroni corrected for multiple comparison,  $p < 0.001$ ), where power in epochs from epileptic group was lower than controls.

There was no significant correlation between this power and number of seizures per day in this region (Pearson correlation,  $p > 0.3$ ). In comparison of this power for different regions, in control animals the only significant difference was found between power of CA3 and EC, where EC was stronger than CA3 (Kruskall-Wallis test, Den's post hoc,  $p < 0.001$ ). In epileptic animals, we had higher power in EC compared to all other regions (Kruskall-Wallis test, Den's post hoc,  $p < 0.001$ ).

We also checked the power in ripple band. Again, DG was the only region with significantly different power between groups, but this time higher in epileptic (Kruskall-Wallis test, Bonferroni corrected for multiple comparison,  $p < 0.001$ ). In comparison of this power for different regions, in control animals only subiculum was stronger than EC (Kruskall-Wallis test, Den's post hoc,  $p < 0.01$ ), and in epileptic animals, power in DG was stronger than CA3 and EC (Kruskall-Wallis test, Den's post hoc,  $p < 0.001$ ).

### 3.3 Phase-amplitude coupling

As already mentioned, all PAC analysis was derived from data epochs of non-REM sleep, during interictal periods at least 1 hour apart from seizures. Our objective was to research new signal markers of epileptogenicity away from seizures. Sleep was a period of particular interest because of signal quality (no movement) and the presence of dominant slow oscillations, as frequency-for-phase candidates.

Figure 3A shows the EEG recorded from an epileptic animal that included ripple-band oscillations (80-200 Hz). The amplitude of oscillations in the ripple band was coupled to the phase of background slow-wave oscillations. Figure 3B reveals phase amplitude coupling in the time-frequency domain of this sample trace. Akin to Canolty et al. (2006), we obtained the time-frequency decompositions of raw EEG epoch (10 min). It was then averaged time-locked to each trough of the dominant slow oscillation (here 0.7 Hz). The top panel shows the normalized average time-frequency map (using logarithmic scale for frequency), and the bottom panel indicates the raw EEG epoch averaged about the trough of the 0.7Hz cycle. This confirmed that the power of faster oscillations was indeed modulated by the phase of the slow rhythm. As shown in figure 3C, our PAC analyses covered high-frequency candidates in 20-250 Hz range. Systematic investigation of slow-to-fast PAC coupling over the frequency ranges of interest revealed that coupling strength was overall stronger in specific frequency bands in the epileptic group compared to controls (Fig. 3C). The plots illustrated in panels B and C of figure 3 indicate that PAC in the analyzed data was not caused by wide-band non-oscillatory activity, but presumably by band-limited ripple oscillations.

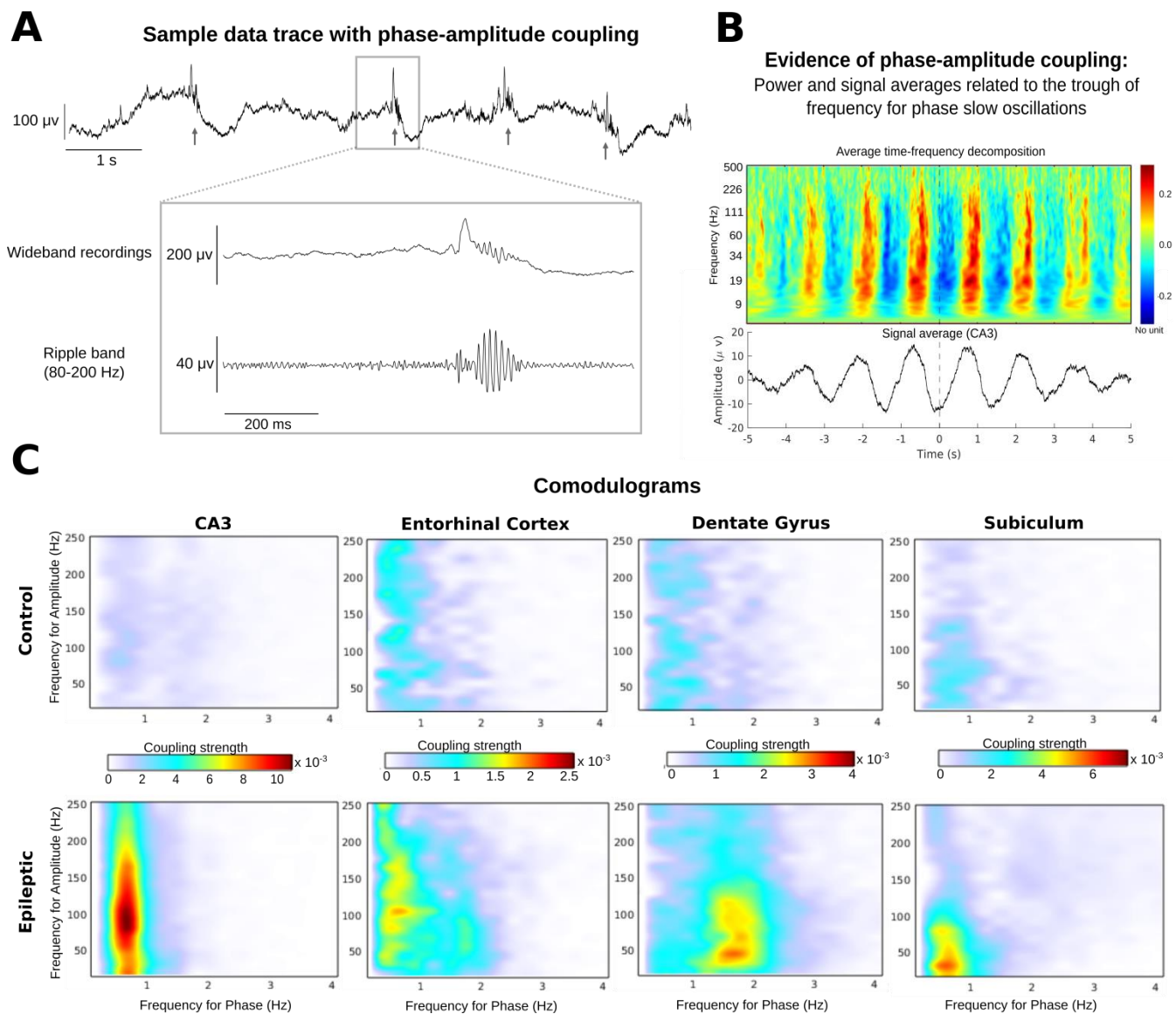


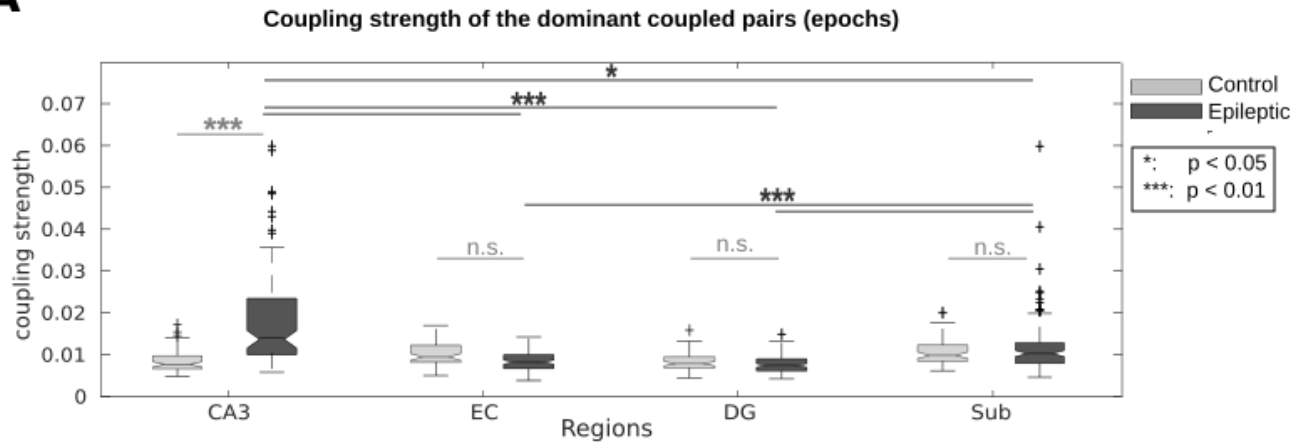
**Figure 3. Phase-amplitude coupling in EEG recordings.** **A:** Sample EEG trace from CA3 of an epileptic animal showing that oscillations in the ripple frequency band (80 - 200 Hz) are modulated by the phase of slow-wave fluctuations (signal polarity is negative up). **B:** Visualization of phase-amplitude coupling in the sample data trace shown in panel A: top panel plots the normalized time-frequency decompositions of EEG signal epoch time-locked averaged with respect to the troughs of the dominant slow oscillation (here 0.7 Hz); the bottom panel plots the corresponding averaged EEG signal (CA3). **C:** Average comodulogram representations of phase-amplitude coupling between slow (0.18 - 4 Hz) and fast (20 - 250 Hz) oscillations, in the control (top row) and epileptic (bottom row) groups. A comodulogram is a two-dimensional representation of the strength of PAC coupling between pairs of oscillatory signal components: frequency



for phase  $f_P$  values are along the x-axis, and frequency for amplitude  $f_A$  values are along the y-axis. The strength of PAC coupling for each  $(f_P, f_A)$  pair is color-coded.

The maximum PAC coupling strength across all  $(f_P, f_A)$  tested frequency pairs was identified for each epoch and recording site, and compared between groups (Fig. 4A). We found that cross-frequency coupling in CA3 was stronger in epileptic animals compared to controls (Kruskall-Wallis test:  $\chi^2(1,36) = 46.3$ , Bonferroni corrected,  $p < 0.001$ ). In the epileptic group, PAC was also stronger in CA3 compared to other regions (Kruskall-Wallis test:  $\chi^2(3, 308) = 81.35$ , post-hoc Dunn's test for pairwise comparison:  $p < 0.001$  compared to EC and DG,  $p = 0.017$  compared to subiculum). The subiculum was the region with the second strongest PAC coupling values (post-hoc Dunn's test,  $p < 0.001$ ). In the control group, PAC was weaker in CA3 and DG than in EC and subiculum (post-hoc Dunn's test for pairwise comparison:  $p < 0.01$ ). We also found that the PAC coupling strength in CA3 and subiculum was positively correlated with the number of seizures per day, across all data epochs from the epileptic group (Pearson's correlation, CA3:  $\rho = 0.44$ , number of epochs = 78,  $p < 0.001$ ; Sub:  $\rho = 0.41$ , number of epochs = 78,  $p < 0.001$ , Fig. 4B). There was no relationship between daily seizure count and coupling strength in the other recorded regions ( $p > 0.10$ ).

**A**



**B**

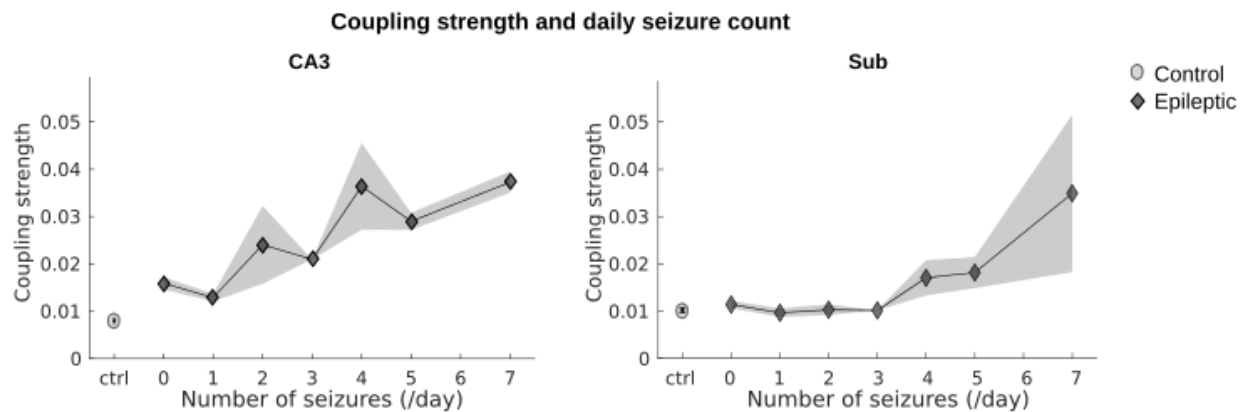
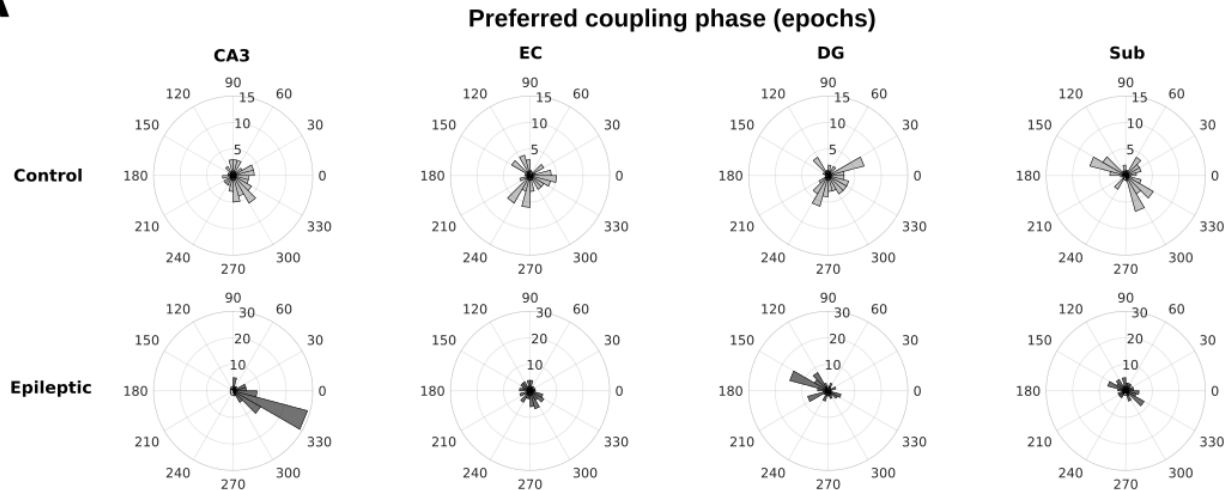


**Figure 4. PAC coupling strength. A:** Strength of PAC coupling in each group and at each recording site. In epileptic animals, PAC was stronger in CA3, followed by the subiculum (Kruskal-Wallis test:  $\chi^2(1,36) = 46.3$ , post-hoc Dunn's test for pairwise comparison:  $p < 0.05$ ). PAC coupling only in CA3 was stronger in epileptic animals than in controls (Kruskal-Wallis test:  $\chi^2(3, 308) = 81.35$ , Bonferroni corrected,  $p < 0.001$ ). **B:** PAC coupling strengths across all data epochs from epileptic group were positively correlated with the number of seizures per day in CA3 (left, Pearson's correlation,  $\rho = 0.44$ , number of epochs = 78,  $p < 0.001$ ) and Sub (right, Pearson's correlation,  $\rho = 0.41$ , number of epochs = 78,  $p < 0.001$ ).

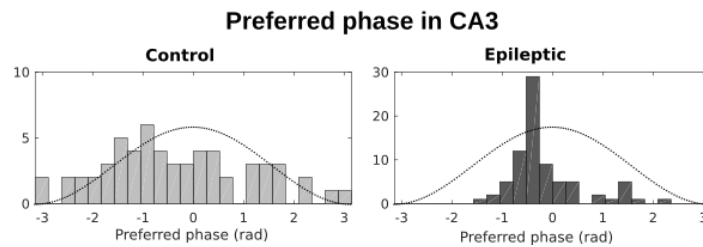
We did not find a monotonic positive relation between the power of slow oscillations and PAC strength measures (Pearson correlation:  $\rho_s < 0$ ,  $|\rho_s| < 0.06$ ,  $p > 0.49$ ). Therefore, we can safely assume that the PAC effects reported were not spuriously produced by harmonics in the electrophysiological waveforms (Jensen et al., 2016).

We also investigated whether the fast oscillatory bouts were generated at consistently preferred phase angles of the underlying slow-wave oscillations across all animals tested. Figure 5A shows the circular histograms of the PAC coupling phases, at each recording site and in both groups. We found preferred phase angles for PAC coupling, except in EC in controls (Rayleigh's test for non-uniformity, Bonferroni-corrected,  $p < 0.01$ ). CA3 was the only recording site where both 1) PAC coupling was stronger in epileptic animals than in controls, and 2) fast oscillations occurred around one preferred phase angle of the underlying slow waves. Therefore, we performed detailed analyses of PAC phase angles in CA3, and found that in both control and epileptic animals, fast oscillations occurred preferentially over the ascending phase of the slow-wave oscillation (mean phase angle in controls:  $-0.53$  rad, in epileptic animals:  $-0.60$  rad). The observed mean phase angle was not significantly different between the two groups (Watson-Williams multi-sample test for equal means,  $F(1,136)=0.08$ ,  $p=0.77$ ). In epileptic animals however, we found that the distribution of preferred phases of PAC coupling was unimodal and substantially more present over the ascending phase of the slow oscillation than in controls (Fig. 5B). Overall, the fast oscillatory PAC events occurred preferentially at the transition phase between the trough and peak of the slow oscillations associated with NREM sleep (Fig. 5C). The preferred phase concentration of fast oscillations towards the end of the transition between the trough and peak of concurrent slow oscillations, are consistent with previous reports in which different signal analysis methods were used to analyze human EEG data (Frauscher et al., 2015; Amiri et al., 2016; Song et al, 2017).

**A**



**B**



**C**

**Schematic of preferred phase in CA3**

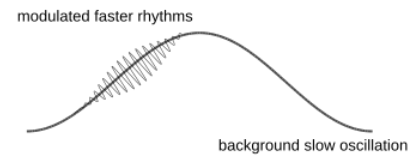


**Figure 5. Distributions of the phase of fast oscillatory activity coupled to slow-wave oscillations. A:** Polar plots show the preferred phase of fast oscillatory activity along the cycle of slow oscillations, across all epochs, for all recording sites and both groups (in degrees angle). Note that in all regions except EC in control animals, the distribution of PAC phase angles was not uniform (Rayleigh's test for non-uniformity, Bonferroni-corrected,  $p < 0.01$ ) **B:** Histogram of observed coupling phase angles in CA3 along the cycle of the slow oscillatory signal, for control and epileptic animals (in radian). The distribution was more expressed towards the end of the ascending phase of the slow oscillatory cycle in epileptic animals. **C:** Schematic illustration of the observed phase and amplitude PAC effects: stronger bouts of fast rhythmic activity occurred consistently and preferentially towards the end of the ascending phase of the underlying slow-wave oscillations in CA3 of the epilepsy group.

## 4 Discussion

Our study emphasizes multiple aspects of NREM sleep polyrhythmic activity in the seizure onset zone, in the pilocarpine animal model of MTLE: 1) at all recording sites, we confirmed the expression of PAC: the amplitude of fast oscillations above 20Hz was modulated by the phase of an underlying slow wave below 4Hz ; 2) this coupling was stronger in the CA3 region of epileptic animals compared to controls; 3) PAC strength in CA3 was positively correlated with the number of seizures per day; and 4) in CA3, high-frequency (50-180 Hz) oscillations occurred preferentially towards the end of the transition between the trough and peak of the underlying slow cycles ( $< 1$  Hz). Our results confirm that PAC is a ubiquitous phenomenon in electrophysiology (Baillet, 2017; Buzsáki and Wang, 2012; Canolty and Knight, 2010). However, they also reveal that PAC signal parameters, such as coupling strength and phase, are relevant to understand the properties of epileptic networks in MTLE. Our findings also emphasize that stronger PAC coupling in the seizure onset zone is related to seizure occurrence.

By extension of the communication through coherence hypothesis (Fries, 2015), it has been proposed that phase-amplitude coupling may be a signal marker of information transfer from large-scale cellular networks to small-scale fast processing networks engaged in effective synaptic modification (Canolty and Knight, 2010). Rodent studies of the mesial temporal regions engaged in working memory processes have shown how PAC may enable multiplexed signal communication between sub-regions of the hippocampus and adjacent structures (Colgin, 2016). Recent imaging work of the electrophysiology of the human resting state also points at the possible role of PAC as a mechanism for large-scale network communication (Florin and Baillet, 2015). PAC parameters are related to the dynamics of network excitability in neural assemblies (Buzsáki and Wang, 2012). For this reason, they are pertinent measures of electrophysiological manifestations of neurological diseases and syndromes that primarily or secondarily affect neural excitability. For instance, early, pre-symptomatic reductions of PAC coupling were observed *in vivo* in the temporal regions of a mouse model of Alzheimer's disease (Goutagny et al., 2013). Alternatively, strong PAC coupling was found in the motor cortex of Parkinson's patients (van Wijk et al, 2016).

We showed here that fast oscillations, essentially in the gamma-ripple band (50-180 Hz), were modulated in amplitude by the phase of slow-wave oscillations ( $< 1$  Hz) in all regions, both in controls and epileptic animals. Our data are in line with previous studies showing strong PAC coupling between the gamma band and slow-wave oscillations in rodents (Andino-Pavlovsky et al., 2017; López-Azcárate et al., 2013), primates (Steriade et al., 1996; Isomura et al., 2006; Takeuchi et al., 2015) and humans (Monto et al., 2008).

To the best of our knowledge, our study is the first to measure phase-amplitude coupling in the temporal lobe after a pilocarpine-induced SE, between the gamma-ripple band and slow-wave oscillations. Epileptic animals showed stronger PAC coupling in the CA3 area, which is often identified as a seizure onset zone in the pilocarpine model of MTLE (Lévesque et al., 2012; Behr et al., 2017; Toyoda et al., 2013). Therefore, our observations are in agreement with previous reports showing strong PAC in the seizure onset zone of epileptic patients (Amiri et al., 2016; Nariai et al., 2011; Weiss et al., 2013; Ibrahim et al., 2014; Guirgis et al., 2015; Weiss et al., 2016). Taken together, these results are consistent with the idea that large networks of neurons fire in synchrony, and produce local-field oscillatory signals in the gamma ripple band that are triggered by slow-wave oscillations. Such fast signals were previously found in the seizure onset zone of epileptic patients (Medvedev et al., 2011; Urrestarazu et al., 2011), with slow-wave oscillations ( $< 1$  Hz) modulating these faster oscillatory signal components (Frauscher et al., 2015). Widespread high-amplitude slow waves are prominent during sleep and could facilitate the expression of such high-frequency activity (Frauscher et al., 2015; Nazer and Dickson, 2009). The mechanisms of generation of high-frequency activity facilitated by slow-wave oscillations remain unclear. Partial evidence suggests that slow-wave oscillations enhance synaptic excitability and hyper-excitability, which would in turn facilitate the development of pathological hyper-synchrony, and eventually epileptiform activity (Nazer and Dickson, 2009; Schall et al., 2008; Wolansky et al., 2006).

We also found that PAC coupling strength in CA3 and subiculum was positively related to seizure occurrence, with stronger PAC coupling associated to high seizure rates. This is presumably to the first report of such association between seizures occurring after SE and PAC coupling strength in

temporal regions. These findings are in line with the hypothesis that episodes of enhanced excitability - marked in the EEG by stronger coupling between gamma-ripple band activity and slow-wave oscillations - are associated with a higher probability of seizure occurrence. Our data are also in agreement with previous evidence showing that interictal spikes are coupled to high-frequency activity in CA3 during episodes of high seizure activity in the pilocarpine model of MTLE (Behr et al., 2015; Lévesque et al., 2011). The subiculum was also previously described as the onset zone of spontaneous seizures in some cases of the pilocarpine model of MTLE (Lévesque et al, 2012; Toyoda et al, 2013). We may therefore assume that changes in PAC in the seizure onset zone reflect time-windows during which neuronal networks undergo substantial changes in neuronal network excitability.

Furthermore, we found that high-frequency oscillations in CA3 occurred preferentially towards the end of the phase transition between troughs and peaks of slow-wave oscillations. Several previous reports pointed at the influence of the coupling phase in the registration of perceptual items by brain systems (Jensen and Colgin, 2007; Gibbs et al., 2016). In epilepsy, a recent study suggested that the phase of occurrence of high-frequency oscillations may be used to distinguish physiological from pathological events (Song et al., 2017). Our findings are concordant with this relatively scarce literature published so far. However, one limitation of our study is that we did not use a surface reference electrode, which would have facilitated the registration of the slow-wave peaks and troughs we observed with the actual up and down states of NREM sleep. Nevertheless, we followed the guidelines published by Ellenrieder et al. (2016) for slow-wave signal interpretation under similar circumstances. Moreover, our data showing a preferred coupling phase towards the end of the transition from slow-wave troughs to peaks are concordant with previous reports on epileptic PAC in human recordings (Frauscher, et al., 2015; Amiri et al., 2016; Song et al., 2017).

In this study, we report on data epochs exclusively from NREM sleep. The rationale is twofold: 1) Contrarily to our data from other sleep stages and wakefulness, NREM sleep data showed a dominant slow oscillation throughout epochs, which we considered a conservative requisite for measuring PAC; 2) interictal NREM sleep produced the lowest rate of movement artefacts, compared to active wakefulness, which was a factor of data quality in support of our findings. Subsequent

research would be required to investigate whether similar PAC signal markers of epileptogenicity would be present during wakefulness and other sleep stages. We also look forward to further PAC studies of the transition between interictal and ictal status. Such research may clarify the physiological mechanisms and circuits involved in seizure activity.

Taken together, our results indicate that measures of phase-amplitude coupling between the phase of slow-wave oscillations and the amplitude of local gamma-ripple band oscillations, are indicative of pathological network activity in the seizure onset zone of pilocarpine-treated epileptic animals. These findings emphasize the potential role of PAC measures as a signal marker of epilepsy. We also anticipate that PAC measures will contribute to improve our understanding of how polyrhythmic brain activity structures the neural dynamics of communication within and between brain systems, and how it is impaired during epileptogenesis and around seizure occurrence. Future studies shall consider producing histological analyses in addition to electrophysiological recordings, to further relate the observed PAC signal markers with anticipated structural and morphological changes in tissues.



## References

- Alvarado-Rojas, C., Valderrama, M., Fouad-Ahmed, A., Feldwisch-Drentrup, H., Ihle, M., Teixeira, C., Sales, F., Schulze-Bonhage, A., Adam, C., Dourado, A., et al. Slow modulations of high-frequency activity (40–140 Hz) discriminate preictal changes in human focal epilepsy. *Scientific reports*, 4, 2014.
- Amiri, M., Frauscher, B., and Gotman, J. Phase-amplitude coupling is elevated in deep sleep and in the onset zone of focal epileptic seizures. *Frontiers in Human Neuroscience*, 10, 2016.
- Andino-Pavlovsky V, Souza AC, Scheffer-Teixeira R, Tort AB, Etchenique R, Ribeiro S. Dopamine Modulates Delta-Gamma Phase-Amplitude Coupling in the Prefrontal Cortex of Behaving Rats. *Frontiers in neural circuits*, 11, 2017.
- Aru, J., Aru, J., Priesemann, V., Wibral, M., Lana, L., Pipa, G., Singer, W., and Vicente, R. Untangling cross-frequency coupling in neuroscience. *Current opinion in neurobiology*, 31: 51–61, 2015.
- Avoli, M., De Curtis, M., Gnatkovsky, V., Gotman, J., Köhling, R., Lévesque, M., Manseau, F., Shiri, Z., and Williams, S. Specific imbalance of excitatory/inhibitory signaling establishes seizure onset pattern in temporal lobe epilepsy. *Journal of neurophysiology*, 115 (6): 3229–3237, 2016.
- Baillet, S. Magnetoencephalography for brain electrophysiology and imaging. *Nature Neuroscience*, 20 (3): 327–339, 2017.
- Behr C, Lévesque M, Ragsdale D, Avoli M. Lacosamide modulates interictal spiking and high-frequency oscillations in a model of mesial temporal lobe epilepsy. *Epilepsy research*, 30;115:8-16, 2015.
- Behr C, Lévesque M, Stroh T, and Avoli M. Time-dependent evolution of seizures in a model of mesial temporal lobe epilepsy. *Neurobiology of Disease*, 106:205-13, 2017.
- Blume WT., and Parrent AG. Assessment of patients with intractable epilepsy for surgery. *Advances in Neurology*, 97: 537-48, 2006.
- Bortel A, Lévesque M, Biagini G, Gotman J, Avoli M. Convulsive status epilepticus duration as determinant for epileptogenesis and interictal discharge generation in the rat limbic system. *Neurobiology of disease*, 40(2):478-89, 2010.

- Bragin, A., Wilson, C. L., Almajano, J., Mody, I., and Engel, J. High-frequency oscillations after status epilepticus: Epileptogenesis and seizure genesis. *Epilepsia*, 45 (9): 1017–1023, 2004.
- Bragin, A., Benassi, S. K., and Engel, J. Patterns of the up–down state in normal and epileptic mice. *Neuroscience*, 225: 76–87, 2012.
- Buzsáki, G. and Wang, X.-J. Mechanisms of gamma oscillations. *Annual review of neuroscience*, 35: 203–225, 2012.
- Canolty, R. T. and Knight, R. T. The functional role of cross-frequency coupling. *Trends in cognitive sciences*, 14 (11): 506, 2010.
- Cendes, F., Andermann, F., Dubeau, F., Gloor, P., Evans, A., Jones-Gotman, M., Olivier, A., Andermann, E., Robitaille, Y., Lopes-Cendes, I., et al. Early childhood prolonged febrile convulsions, atrophy and sclerosis of mesial structures, and temporal lobe epilepsy an mri volumetric study. *Neurology*, 43 (6): 1083–1083, 1993.
- Cole, S. R. and Voytek, B. Brain oscillations and the importance of waveform shape. *Trends in cognitive sciences*, 2017.
- Colgin, L. L. Rhythms of the hippocampal network. *Nat Rev Neurosci*, 2016, 17, 239-249
- Colic S, Lang M, Wither RG, Eubanks JH, Liang Z, Bardakjian BL. Low frequency-modulated high frequency oscillations in seizure-like events recorded from in-vivo MeCP2-deficient mice. *InEngineering in Medicine and Biology Society (EMBC), 35th Annual International Conference of the IEEE*, 985-988, 2013.
- Curia G, Longo D, Biagini G, Jones RSG, Avoli M. The pilocarpine model of temporal lobe epilepsy. *Journal of neuroscience methods*, 172(2): 143-157, 2008.
- Ellenrieder N, Frauscher B, Dubeau F, Gotman J. Interaction with slow waves during sleep improves discrimination of physiologic and pathologic high- frequency oscillations (80–500 Hz). *Epilepsia*, 57(6):869-78, 2016.
- Engel, J. Report of the ILAE classification core group. *Epilepsia* 47(9): 1558-1568, 2006.

- Engel, J., McDermott, M. P., Wiebe, S., Langfitt, J. T., Stern, J. M., Dewar, S., Sperling, M. R., Gardiner, I., Erba, G., Fried, I., et al. Early surgical therapy for drug-resistant temporal lobe epilepsy: a randomized trial. *Jama*, 307 (9): 922–930, 2012.
- Florin E, Baillet S. The brain's resting-state activity is shaped by synchronized cross-frequency coupling of neural oscillations. *Neuroimage*, 111:26-35, 2015.
- Frauscher, B., von Ellenrieder, N., Ferrari-Marinho, T., Avoli, M., Dubeau, F., and Gotman, J. Facilitation of epileptic activity during sleep is mediated by high amplitude slow waves. *Brain*, 138 (6): 1629–1641, 2015.
- Frauscher, B., Bartolomei, F., Kobayashi, K., Cimbalka, J., Klooster, M. A., Rampp, S., Otsubo, H., Höller, Y., Wu, J. Y., Asano, E., et al. High-frequency oscillations: The state of clinical research. *Epilepsia*, 58(8):1316-29, 2017.
- French, J., Williamson, P., Thadani, V., Darcey, T., Mattson, R., Spencer, S., and Spencer, D. Characteristics of medial temporal lobe epilepsy: I. results of history and physical examination. *Annals of neurology*, 34 (6): 774–780, 1993.
- Fries P. Rhythms for cognition: communication through coherence. *Neuron*, 88(1): 220-35, 2015.
- James, G., Witten D., Hastie T., and Tibshirani R., An introduction to statistical learning. New York: springer; 2013.
- Gao, R. and Penzes, P. Common mechanisms of excitatory and inhibitory imbalance in schizophrenia and autism spectrum disorders. *Current molecular medicine*, 15 (2): 146–167, 2015.
- Gerber, E. M., Sadeh, B., Ward, A., Knight, R. T., and Deouell, L. Y. Non-sinusoidal activity can produce cross-frequency coupling in cortical signals in the absence of functional interaction between neural sources. *PloS one*, 11 (12): e0167351, 2016.
- Gips B, Eerden JP, Jensen O. A biologically plausible mechanism for neuronal coding organized by the phase of alpha oscillations. *European Journal of Neuroscience*. 44(4):2147-61, 2016.
- Gloor, Pierre. The temporal lobe and limbic system. *Oxford University Press*, USA, 1997.
- Goffin K, Nissinen J, Van Laere K, Pitkänen A. Cyclicity of spontaneous recurrent seizures in pilocarpine model of temporal lobe epilepsy in rat. *Experimental neurology*, 205(2):501-5, 2007.

- Gogolla, N., LeBlanc, J. J., Quast, K. B., Südhof, T. C., Fagiolini, M., and Hensch, T. K. Common circuit defect of excitatory-inhibitory balance in mouse models of autism. *Journal of neurodevelopmental disorders*, 1 (2): 172, 2009.
- Gotman J, and Marciani MG. Electroencephalographic spiking activity, drug levels, and seizure occurrence in epileptic patients. *Annals of neurology*. 17(6):597-603, 1985.
- Goutagny, R.; Gu, N.; Cavanagh, C.; Jackson, J.; Chabot, J.-G.; Quirion, R.; Krantic, S. & Williams, S. Alterations in hippocampal network oscillations and theta-gamma coupling arise before A $\beta$  overproduction in a mouse model of Alzheimer's disease. *Eur J Neurosci*, 37: 1896-1902, 2013.
- Guirgis, M., Chinvarun, Y., del Campo, M., Carlen, P. L., and Bardakjian, B. L. Defining regions of interest using cross-frequency coupling in extratemporal lobe epilepsy patients. *Journal of neural engineering*, 12 (2): 026011, 2015.
- Hufnagel, A., Dümpelmann, M., Zentner, J., Schijns, O., and Elger, C. Clinical relevance of quantified intracranial interictal spike activity in presurgical evaluation of epilepsy. *Epilepsia*, 41 (4): 467–478, 2000.
- Ibrahim, G. M., Wong, S. M., Anderson, R. A., Singh-Cadieux, G., Akiyama, T., Ochi, A., Otsubo, H., Okanishi, T., Valiante, T. A., Donner, E., et al. Dynamic modulation of epileptic high frequency oscillations by the phase of slower cortical rhythms. *Experimental neurology*, 251: 30–38, 2014.
- Isomura, Y., Sirota, A., Özen, S., Montgomery, S., Mizuseki, K., Henze, D. A., and Buzsáki, G. Integration and segregation of activity in entorhinal-hippocampal subregions by neocortical slow oscillations. *Neuron*, 52 (5): 871–882, 2006.
- Jallon, P., Epilepsy in developing countries. *Epilepsia*, 38(10), 1143-1151, 1997.
- Jacobs, J., Zijlmans, M., Zelmann, R., Chatillon, C.-É., Hall, J., Olivier, A., Dubeau, F., and Gotman, J. High-frequency electroencephalographic oscillations correlate with outcome of epilepsy surgery. *Annals of neurology*, 67 (2): 209–220, 2010.
- Jensen, O., Spaak, E., and Park, H. Discriminating valid from spurious indices of phase-amplitude coupling. *eNeuro*, 3 (6): ENEURO–0334, 2016.
- Karunakaran S, Grasse DW, Moxon KA. Role of CA3 theta-modulated interneurons during the transition to spontaneous seizures. *Experimental neurology*. 283: 341-52, 2016.

- Kehrer, C., Maziashvili, N., Dugladze, T., and Gloveli, T. Altered excitatory-inhibitory balance in the nmda-hypofunction model of schizophrenia. *Frontiers in molecular neuroscience*, 1, 2008.
- Lange HH, Lieb JP, Engel J, and Crandall PH. Temporo-spatial patterns of pre-ictal spike activity in human temporal lobe epilepsy. *Electroencephalography and clinical neurophysiology*. 56(6): 543-55, 1983.
- Lévesque M, Bortel A, Gotman J, and Avoli M. High-frequency (80–500Hz) oscillations and epileptogenesis in temporal lobe epilepsy. *Neurobiology of disease*, 42(3): 231-41, 2011.
- Lévesque M, Salami P, Gotman J, and Avoli M. Two seizure-onset types reveal specific patterns of high-frequency oscillations in a model of temporal lobe epilepsy. *Journal of Neuroscience*, 32(38): 13264-72, 2012.
- Lévesque M, Behr C, and Avoli M. The anti-ictogenic effects of levetiracetam are mirrored by interictal spiking and high-frequency oscillation changes in a model of temporal lobe epilepsy. *Seizure*, 25:18-25, 2015.
- López-Azcárate J, Nicolás MJ, Cordon I, Alegre M, Valencia M, Artieda J. Delta-mediated cross-frequency coupling organizes oscillatory activity across the rat cortico-basal ganglia network. *Frontiers in neural circuits*, 7, 2013.
- Lozano-Soldevilla, D., ter Huurne, N., and Oostenveld, R. Neuronal oscillations with non-sinusoidal morphology produce spurious phase-to-amplitude coupling and directionality. *Frontiers in computational neuroscience*, 10, 2016.
- Martin, B. S. and Kapur, J. A combination of ketamine and diazepam synergistically controls refractory status epilepticus induced by cholinergic stimulation. *Epilepsia*, 49 (2): 248–255, 2008.
- McDonald, J. W., Garofalo, E. A., Hood, T., Sackellares, J. C., Gilman, S., McKeever, P. E., Troncoso, J. C., and Johnston, M. V. Altered excitatory and inhibitory amino acid receptor binding in hippocampus of patients with temporal lobe epilepsy. *Annals of neurology*, 29 (5): 529–541, 1991.
- Medvedev AV, Murro AM, Meador KJ. Abnormal interictal gamma activity may manifest a seizure onset zone in temporal lobe epilepsy. *International journal of neural systems*, 21(2): 103-114, 2011.
- Monto S, Palva S, Voipio J, Palva JM. Very slow EEG fluctuations predict the dynamics of stimulus detection and oscillation amplitudes in humans. *Journal of Neuroscience*, 28(33): 8268-8272, 2008.

- Nariai, H., Matsuzaki, N., Juhász, C., Nagasawa, T., Sood, S., Chugani, H. T., and Asano, E. Ictal high-frequency oscillations at 80–200 hz coupled with delta phase in epileptic spasms. *Epilepsia*, 52(10), 2011.
- Nazer F, Dickson CT. Slow oscillation state facilitates epileptiform events in the hippocampus. *Journal of neurophysiology*, 102(3): 1880-1889, 2009.
- Palop, J. J., Chin, J., Roberson, E. D., Wang, J., Thwin, M. T., Bien-Ly, N., Yoo, J., Ho, K. O., Yu, G.-Q., Kreitzer, A., et al. Aberrant excitatory neuronal activity and compensatory remodeling of inhibitory hippocampal circuits in mouse models of alzheimer's disease. *Neuron*, 55 (5): 697–711, 2007.
- Pitsch J, Becker AJ, Schoch S, Müller JA, Curtis M, Gnatkovsky V. Circadian clustering of spontaneous epileptic seizures emerges after pilocarpine- induced status epilepticus. *Epilepsia*, 58(7):1159-71, 2017.
- Paxinos, G. and Watson, C. The rat brain in stereotaxic coordinates. vol, 1998.
- Rodin, E., Constantino, T., and Bigelow, J. Interictal infraslow activity in patients with epilepsy. *Clinical Neurophysiology*, 125 (5): 919–929, 2014.
- Samiee, S. and Baillet, S. Time-resolved phase-amplitude coupling in neural oscillations. *NeuroImage*, 159:270-279, 2017.
- Salami P, Lévesque M, Benini R, Behr C, Gotman J, and Avoli M. Dynamics of interictal spikes and high-frequency oscillations during epileptogenesis in temporal lobe epilepsy. *Neurobiology of disease*, 31(67):97-106, 2014.
- Salanova, V., et al. "Reevaluation of surgical failures and the role of reoperation in 39 patients with frontal lobe epilepsy." *Epilepsia* 35(1): 70-80, 1994.
- Schall KP, Kerber J, Dickson CT. Rhythmic constraints on hippocampal processing: state and phase-related fluctuations of synaptic excitability during theta and the slow oscillation. *Journal of neurophysiology*, 99(2): 888-899, 2008
- Song I, Orosz I, Chervoneva I, Waldman ZJ, Fried I, Wu C, Sharan A, Salamon N, Gorniak R, Dewar S, Bragin A. Bimodal coupling of ripples and slower oscillations during sleep in patients with focal epilepsy, *Epilepsia*, 2017.

- Spencer, S. S. and Spencer, D. D. Entorhinal-hippocampal interactions in medial temporal lobe epilepsy. *Epilepsia*, 35 (4): 721–727, 1994.
- Spencer S., and Huh L. Outcomes of epilepsy surgery in adults and children. *The Lancet Neurology*, 7(6):525-537, 2008.
- Steriade M, Amzica F, Contreras D. Synchronization of fast (30-40 Hz) spontaneous cortical rhythms during brain activation. *Journal of Neuroscience*, 16(1): 392-417, 1996.
- Tadel, F., Baillet, S., Mosher, J. C., Pantazis, D., and Leahy, R. M. Brainstorm: a user-friendly application for meg/eeeg analysis. *Computational intelligence and neuroscience*, 2011:2018, 2011.
- Takeuchi S, Mima T, Murai R, Shimazu H, Isomura Y, Tsujimoto T. Gamma oscillations and their cross-frequency coupling in the primate hippocampus during sleep. *Sleep*, 38(7): 1085-1091, 2015.
- Tort, A. B., Komorowski, R., Eichenbaum, H., & Kopell, N. Measuring phase-amplitude coupling between neuronal oscillations of different frequencies. *Journal of neurophysiology*, 104(2): 1195-1210, 2010.
- Toyoda I, Bower MR, Leyva F, Buckmaster PS. Early activation of ventral hippocampus and subiculum during spontaneous seizures in a rat model of temporal lobe epilepsy. *Journal of Neuroscience*, 33(27): 11100-15, 2013.
- Toyoda I, Fujita S, Thamattoor AK, Buckmaster PS. Unit activity of hippocampal interneurons before spontaneous seizures in an animal model of temporal lobe epilepsy. *Journal of Neuroscience*, 35(16): 6600-6618, 2015.
- Urrestarazu E, Chander R, Dubeau F, Gotman J. Interictal high-frequency oscillations (100–500 Hz) in the intracerebral EEG of epileptic patients. *Brain*, 130(9): 2354-2366, 2007.
- Vanhatalo, S., Palva, J. M., Holmes, M., Miller, J., Voipio, J., and Kaila, K. Infralow oscillations modulate excitability and interictal epileptic activity in the human cortex during sleep. *Proceedings of the National Academy of Sciences of the United States of America*, 101 (14): 5053–5057, 2004.
- van Wijk BC, Beudel M, Jha A, Oswal A, Foltynie T, Hariz MI, Limousin P, Zrinzo L, Aziz TZ, Green AL, Brown P. (2016), Subthalamic nucleus phase–amplitude coupling correlates with motor impairment in Parkinson’s disease. *Clinical Neurophysiology*, 127(4): 2010-2019.

Weiss, S. A., Banks, G. P., McKhann, G. M., Goodman, R. R., Emerson, R. G., Trevelyan, A. J., and Schevon, C. A. Ictal high frequency oscillations distinguish two types of seizure territories in humans. *Brain*, 136(12): 3796-3808., 2013.

Weiss, S A, Alvarado- Rojas C, Bragin A, Behnke E, Fields T, Fried I, Engel J, Staba R. Ictal onset patterns of local field potentials, high frequency oscillations, and unit activity in human mesial temporal lobe epilepsy. *Epilepsia*, 57(1): 111-121, 2016.

Wendling F, Chauvel P, Biraben A, Bartolomei F. From intracerebral EEG signals to brain connectivity: identification of epileptogenic networks in partial epilepsy. *Frontiers in systems neuroscience*, 4, 2010.

Wendling AS, Hirsch E, Wisniewski I, Davanture C, Ofer I, Zentner J, Bilic S, Scholly J, Staack AM, Valenti MP, Schulze-Bonhage A. Selective amygdalohippocampectomy versus standard temporal lobectomy in patients with mesial temporal lobe epilepsy and unilateral hippocampal sclerosis. *Epilepsy research*. 104(1-2):94-104, 2013.

Wiebe, S., Blume, W. T., Girvin, J. P., and Eliasziw, M. A randomized, controlled trial of surgery for temporal-lobe epilepsy. *New England Journal of Medicine*, 345(5): 311-318, 2001.

Wiebe S. Effectiveness and safety of epilepsy surgery: what is the evidence?. *CNS spectrums*, 9(2):120-132, 2004.

Wolansky T, Clement EA, Peters SR, Palczak MA, Dickson CT. Hippocampal slow oscillation: a novel EEG state and its coordination with ongoing neocortical activity. *Journal of Neuroscience*, 26(23): 6213-6229, 2006.

Zhang, R., Ren, Y., Liu, C., Xu, N., Li, X., Cong, F., Ristaniemi, T., and Wang, Y. Temporal-spatial characteristics of phase-amplitude coupling in electrocorticogram for human temporal lobe epilepsy. *Clinical Neurophysiology*, 128(9):1707-1718, 2017.

Zijlmans, M., Jacobs, J., Zelmann, R., Dubeau, F., and Gotman, J. High-frequency oscillations mirror disease activity in patients with epilepsy. *Neurology*, 72 (11): 979–986, 2009.



## Highlights

- An electrophysiology signal marker of epileptogenicity is proposed.
- It measures phase-amplitude coupling between slow and fast oscillations.
- The strength of such coupling is positively correlated with seizure frequency.
- This marker is specific of the seizure onset zone.